Environmental Earth Sciences (2024) 83:465
https://doi.org/10.1007/s12665-024-11771-3

ORIGINAL ARTICLE

Magnetic fabrics of west coast dyke swarm from Deccan volcanic province, Maharashtra, India and their relationship with magma flow direction

B. V. Lakshmi[1] · K. Deenadayalan[1] · A. P. Dimri[1]

Received: 23 November 2023 / Accepted: 20 July 2024 / Published online: 5 August 2024

Abstract
Dykes are one of the primary subvolcanic bodies that transport magma from the shallow magma chamber or from the deep-seated magma reservoir. The mechanism of magma transport and emplacement in dyke swarms can contribute precious details on source and how magma has associated with crustal rocks. Here we are presenting the results obtained from the Anisotropy of magnetic susceptibility (AMS) on their mode of emplacement and to understand magma flow direction. AMS and rock magnetic studies were performed on 33 dykes located on the West coast of Maharashtra, (India) to determine the magma flow direction using magnetic fabric. Thermomagnetic curves and hysteresis loop measurement indicates that titanomagnetite of associated pseudo-single-domain/multi-domain grain sizes are responsible for the magnetic fabrics. Based on the clustering of the principal AMS axes, three types of AMS fabrics were recognized, (i) Normal fabric, interpreted as due to magma flow characterised by clustering of K_1–K_2 axes on the dyke plane and K_3 axes are nearly perpendicular to it, (ii) Inverse fabric with K_2–K_3 plane parallel to the dyke plane and K_3 is perpendicular to it and (iii) Intermediate fabric, with K_1–K_3 axes clustering close to dyke plane. The inclination of the K_1 axis (IK_1) of Normal fabric is the most important to determine the flow of magma for the studied dyke swarm. The IK_1 of the studied dykes were fed dominantly by horizontal ($IK_1 < 30°$), inclined ($30° < IK_1 < 60°$) up to vertical fluxes ($IK_1 > 60°$). These results suggest that the dykes may be closer to the magma source and horizontal magma flow inferred from the dykes reveals source is located further away. The present AMS study along with geophysical, geochemical and petrological study supports the evidence of feeder fed mechanism.

Keywords Anisotropy of magnetic susceptibility · Rock magnetic · Deccan volcanic province · Magma flow · Magnetic fabric · Dyke swarms

Introduction

The Deccan flood basalt province of India is one of the largest lava plateau in the world with a present day aerial extent of 500,000 km^2 (Mahoney 1988). The volcanics attain a maximum thickness of over 3000 m in the sections of Western Ghats along the Indian west coast (Courtillot and Renne 2003). The origin of the Deccan Volcanic Province (DVP) is still debatable. Many workers believed in the plume origin of this volcanism (Morgan 1981; Richards et al. 1989; Campbell and Griffiths 1990), the alternative suggestion is that this volcanism was related to the continental rift zone (Sheth 2005). Whilst there has been a growing consensus as to the genesis of DVP, the alternative model has remained unclear. Numerous dyke swarms within the DVP occur along the west coast of India (Fig. 1) either parallel to the N-S trending Cambay rift or the E-W trending Narmada-Tapati-Satpura lineament (Fig. 1a), only a few dykes deviate from these trends and oriented in NW–SE and NE-SW directions (Deshmukh and Sehgal 1988). These dykes play an important role in determining the magma emplacement mechanism. Anisotropy of magnetic susceptibility (AMS) is one such study that is used to understand the magma flow pattern of dyke swarms.

AMS is the second-rank tensor referred to as the susceptibility tensor. It is defined by the intensity of the applied field (H) to the acquired magnetization (M) of a material through the equation: $M_i = K_{ij}H_j$ (Hrouda 1982; Raposo et al.

✉ B. V. Lakshmi
lakshmi.bv@iigm.res.in

[1] Indian Institute of Geomagnetism, Kalamboli Highway, New Panvel, Navi Mumbai 410218, India

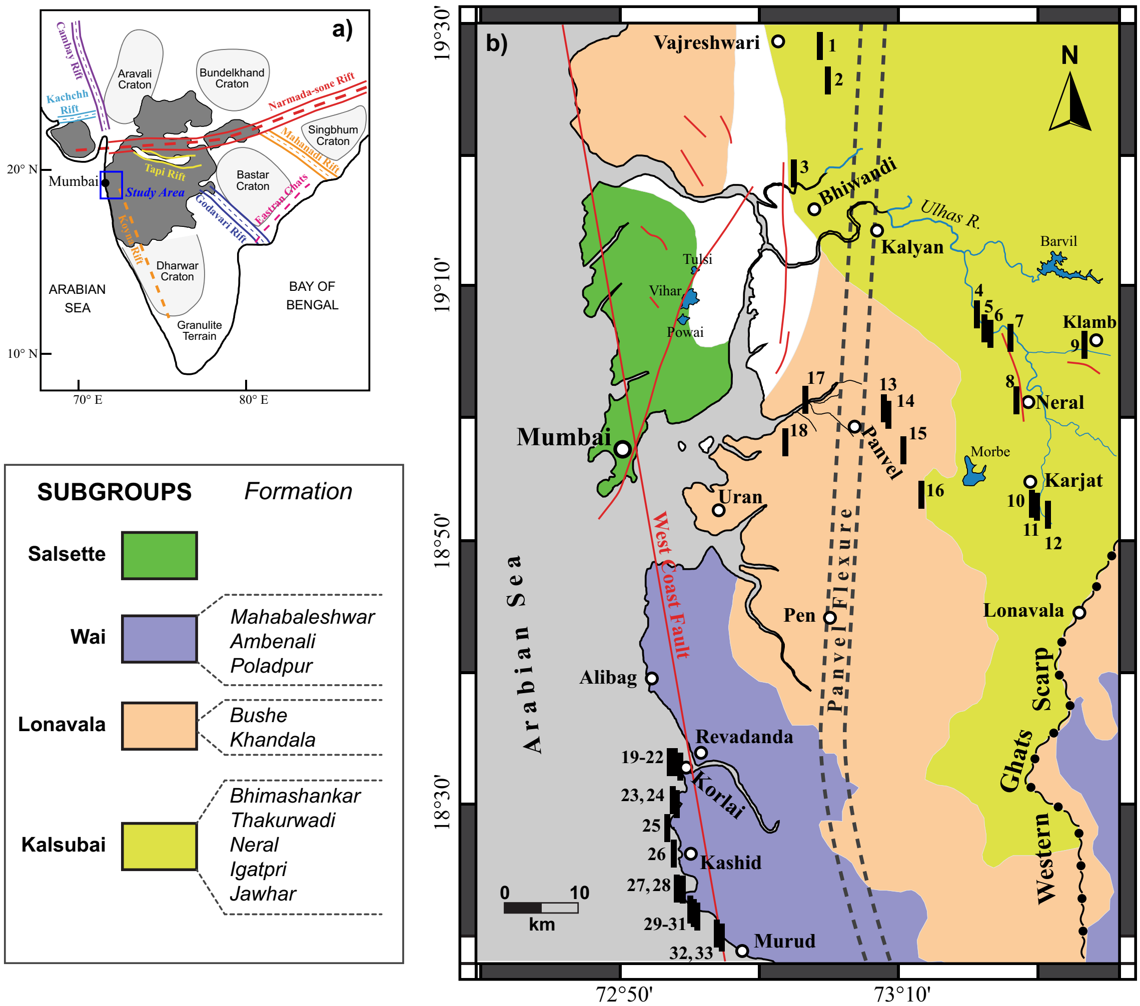

Dyke Numbering: 1. Vajreswari (VRI); 2. Dugurpada (DGA); 3.Biwandi (BNI); 4-8. Neral (NRL1,NRL2, NRL3, NRL4, NRL5); 9. Kalamb (KMB); 10, 11. Sireva (SRA1, SRA2); 12. Nevali (NVI); 13, 14. Chipale (CPE1, CPE2); 15. Shedung (SDG); 16. Panshil (PSL); 17. Belapur (BLR); 18. Ulwe (ULE); 19-22. Korlai (KLI1, KLI2, KLI3, KLI4); 23, 24. Borlai (BLI1, BLI2); 25. Revadanda (RDA); 26. Kashid (KSD); 27, 28. More (MRE1, MRE2); 29-31. Vihoor (VHR1, VHR2, VHR3); 32, 33. Murud (MRD1, MRD2).

Fig. 1 **a** Simplified map of peninsular India showing the major cratons and rift zones (modified after Sheth 2005). **b** Site map showing 33 dyke locations sampled at west coast south, north and NE of Mumbai along with Panvel flexure and flow stratigraphy of Deccan traps (Salsette, Wai, Lonavala and Kalsubai) of Western Ghats escarpment. The black bar represent studied dykes, red lines faults as per Geological Survey of India (District Resource Maps 2001)

2004). AMS tensor can be expressed by three principal axes representing maximum (K_1), intermediate (K_2), and minimum (K_3) susceptibility axes. AMS represents the directional variation of magnetic susceptibility within a material and constitutes the contribution of dia-, para- and ferrimagnetic minerals. The magnetic lineation is represented by the K_1 axis while the pole of the magnetic foliation (the plane formed by K_1 and K_2 axes) is K_3. AMS in rocks carried by Fe-bearing silicate paramagnetic matrix minerals is due to the magnetocrystalline anisotropy and that of ferrimagnetic minerals, AMS corresponds to the shape anisotropy of these minerals. The study of AMS is the most efficient tool to investigate the problems related to petrofabric orientation in rocks, sedimentology, tectonics and igneous process (Khan 1962; Hrouda 1982; Knight and Walker 1988; Rochette et al. 1992; Raposo and D'Argella-Filho 2000; Chadima et al. 2009; Canon-Tapia and Herrero-Bervera 2009). AMS is a complex phenomenon due to the mixed contributions of magnetic minerals and their domain states to the overall anisotropy of a sample (Rochette et al. 1992). The AMS study of dyke swarms has been found to be a very useful tool in determining magma emplacement kinematics (Knight and Walker 1988; Rapalini and Luchi 2000; Roposo et al. 2004).

Throughout the world, AMS studies contributed much to understanding the flow pattern in dyke swarms (Ernst and Baragar 1992; Raposo and Ernesto 1995; Curtis et al.

2008; Pratheesh et al. 2011; Pan et al. 2014; Kumar et al. 2015; Ramesh et al. 2020; Das et al. 2021). Several studies approached to differentiate sedimentary and tectonic fabric in deformed rocks (Tarling and Hrouda 1993; Parés et al. 1999; Borradaile and Jackson 2004; Levi et al. 2014; Maffione et al. 2015; Weinberger et al. 2017; Bradak et al. 2019) and to characterize earthquake- induced deformation features (Levi et al. 2006; Morner and Sun 2008; Font et al. 2010; Lakshmi et al. 2015, 2020; Chao et al. 2017). In India, AMS studies were applied to determine the magma flow direction in dykes (Prasad et al. 1999; Pratheesh et al. 2011; Kumar et al. 2015; Ramesh et al. 2020; Das et al. 2021) and to another geological context also (Nagaraju et al 2008; Mallik et al. 2009; Mamtani et al. 2013; Renjith et al. 2016).

The dyke swarms in the DVP spread over Maharashtra, Gujarat and Madhya Pradesh. Paleomagnetic and geochemical studies on dykes in India have been carried out extensively but AMS on dykes is scanty (e.g. Vandamme et al. 1991; Radhakrishna and Joseph 1993; Powar and Vadetwar 1995; Prasad et al. 1996; Subbarao et al. 1998; Courtillot et al. 2000; Rao 2002; Srivastava 2006; Ray et al. 2007; Chenet et al. 2008). Patil and Arora (2003) published paleomagnetic results of six dykes from Murud, Mumbai. Basavaiah et al. (2018) revised and reported new paleomagnetic results on 33 dykes from the west coast south, north and NE of Mumbai, Maharashtra. Out of 33 dykes investigated, 29 dykes have yielded stable characteristic remanent magnetizations (ChRM) amenable for statistical analysis. Twenty dykes exhibit N-polarity and nine dykes show R-polarity. This study, however, does indicate the possible presence of two more reversals beyond well-established three-Chron magnetostratigraphy. However, no study on AMS of west coast dykes has been investigated so far. In the present study, the AMS was used for the same 33 dykes from Basavaiah et al. (2018), to investigate the significance of magnetic fabrics. Additionally we also provide information on their mode of emplacement and to understand magma flow direction.

Geological setting and sampling

The dyke swarm outcrop in the DVP namely the ENE-WSW trending Narmada-Satpura-Tapi region containing thousands of dykes, the NNW-SSE trending Konkan or west coast dyke swarms and the Western Ghats swarm NE of Mumbai (e.g., Dessai and Viegas 1995; Bondre et al. 2006). These zones are believed to be regions for mafic dyke swarms (e.g., Sheth 2000). Mafic dyke swarms cover areas of 87,000 km^2 in the West Coast belts in the Deccan volcanic province (Deshmukh and Sehgal 1988). The coast-parallel N-S trending dyke swarm extends over 90 km from Mumbai to Murud. These dykes are mainly dolerites of tholeiitic character. The Panvel flexure formed along the west coast as a consequence of late-stage east–west extension that culminated in the post-Deccan rifting and separation of the Seychelles microcontinent (e.g. Dessai and Bertrand 1995; Sheth 1999; Hooper et al. 2010). The area is predominantly occupied by tholeiitic basalts that have been classified as upper Traps (Pascoe 1964). However, from the chemostratigraphic work (Bean et al. 1986) these rocks are included under Poladpur and Ambenali formations of the youngest Wai sub-group of the Deccan basalt group (Subbarao and Hooper 1988) of late Cretaceous to Eocene age (Mahoney 1988). Powar and Vadetwar (1995) suggested that both dykes and flows represent the Poladpur magma type. They confirmed, based on the spatial distribution of the dykes, their close-spaced occurrence, and often restricted thickness that the dykes are hypabyssal intrusives rather than feeders. They also observed that the dykes were emplaced immediately after the outpouring of basalts of Poladpur formation. Based on the field observations, it is suggested that the N-S dykes represent the youngest intrusive phase, while the E-W, NW–SE, and NE-SW dykes are the older intrusive phases within the DVP along the west coast of India.

A total of 33 dykes, west coast south, north, and NE of Mumbai (Fig. 1b, Table 1) were sampled for rock magnetic and AMS studies. The majority of dykes showed tilt angles ranging from 1 to 15°, while few dykes exhibit tilt ~20° (Table 1). Altogether 158 cores, from 33 dykes mostly from the central part of the dykes were drilled in the field using a portable gasoline-powered drill fitted with a water-cooled diamond drill bit (Stihl, USA). The orientation of the core (i.e. azimuth and dip) is determined with an accuracy of ± 2° using a magnetic compass. The orientation device has a non-magnetic slotted tube with an adjustable platform on which a magnetic compass and inclinometer are fitted. A total of 349 standard cylindrical specimens of size 2.5 cm diameter and 2.2 cm length were cut in the laboratory. In the AMS study, magnetic mineralogy and its orientation is a primary step to understanding the type of fabric and mode of flow. We have collected new and fresh samples for AMS and rock magnetic studies and the results are presented in this study.

Experimental details

The measurement of low-field (200 Am^{-1} at 976 Hz) AMS for each specimen was carried out using a MFK1 kappabridge with measurements in 64 directions on three mutually orthogonal planes, using an automatic rotator sample holder. The azimuths and magnitudes of principal susceptibility axes (K_{max}, K_{int}, and K_{min}) were calculated using SUFAR software supplied by AGICO, together with other magnetic anisotropy parameters such as anisotropy ratios, expressed as corrected degree of anisotropy (P′) and shape (T) (Jelínek 1981). The analysis of the AMS data

Table 1 Site location of west coast dykes, Mumbai

Sr. No	Site location	Sample code	Width (m)	Tilt	Strike	Latitude (N)	Longitude (E)
1	Vajreswari	VRI	2.5	–	N30°E	19°28′44.2″	73°03′44.2″
2	Dugurpada	DGA	6.5	–	N1°W	19°26′25.5″	73°04′10.5″
3	Biwandi	BNI	1.0	11°W	N–S	19°18′54.7″	73°01′45.4″
4	Neral	NRL1	5.5	10°W	N20°E	19°07′54.0″	73°15′48.3″
5	Neral	NRL2	33.0	19°E	N30°E	19°06′52.8″	73°16′26.0″
6	Neral	NRL3	20.0	4°W	N15°E	19°06′48.7″	73°16′32.4″
7	Neral	NRL4	15.0	13°W	N35°E	19°06′42.5″	73°16′49.5″
8	Neral	NRL5	18.9	11°E	N10°E	19°01′51.0″	73°18′46.0″
9	Kalamb	KMB	9.0	13°E	N85°E	19°05′32.8″	73°23′15.2″
10	Sireva	SRA1	1.6	10°E	N–S	18°53′19.9″	73°19′46.1″
11	Sireva	SRA2	1.3	11°W	N–S	18°53′19.9″	73°19′46.1″
12	Nevali	NVI	4.3	22°E	N–S	18°52′58.7″	73°20′08.4″
13	Chipale	CPE1	1.9	17°E	N2°E	19°00′15.8″	73°08′51.4″
14	Chipale	CPE2	10.5	14°E	N2°E	19°00′15.8″	73°08′51.4″
15	Shedung	SDG	6.0	18°E	N10°E	18°57′40.8″	73°10′21.4″
16	Panshil	PSL	3.0	12°E	N40°E	18°54′27.0″	73°12′36.1″
17	Belapur	BLR	5.0	17°E	N–S	19°01′19.9″	72°02′54.2″
18	Ulwe	ULE	5.4	16°E	N–S	18°58′08.5″	73°01′28.8″
19	Korlai	KLI1	3.9	13°E	N–S	18°31′57.4″	72°54′27.9″
20	Korlai	KLI2	2.2	5°E	N15°E	18°31′51.2″	72°55′12.8″
21	Korlai	KLI3	1.5	7°W	N–S	18°32′14.9″	72°56′17.9″
22	Korlai	KLI4	1.9	8°E	E–W	18°32′17.2″	72°54′17.8″
23	Borlai	BLI1	1.1	3°E	E–W	18°30′46.3″	72°54′35.8″
24	Borlai	BLI2	2.0	11°E	N–S	18°30′46.2″	72°54′35.4″
25	Revadanda	RDA	3.6	–	N315°W	18°29′44.5″	72°54′15.4″
26	Kashid	KSD	0.7	2°E	N–S	18°25′27.0″	72°54′30.1″
27	More	MRE1	0.6	–	N20°E	18°20′58.4″	72°55′41.1″
28	More	MRE2	1.0	10°W	N–S	18°20′01.0″	72°55′45.4″
29	Vihoor	VHR1	0.6	5°E	N30°E	18°21′01.5″	72°55′47.5″
30	Vihoor	VHR2	0.6	11°E	N45°E	18°21′01.0″	72°55′50.0″
31	Vihoor	VHR3	0.7	2°E	N–S	18°21′01.0″	72°55′50.3″
32	Murud	MRD1	0.2	10°W	N–S	18°18′43.6″	72°57′31.9″
33	Murud	MRD2	4.5	–	N75°E	18°18′56.0″	72°57′21.7″

was performed using the Anisoft 5 software. Detailed rock magnetic experiments were carried out on representative specimens from each dyke in order to determine their main magnetic carrier. Selected samples of each profile were subjected to high-temperature magnetization and hysteresis loop measurements in order to gain further insights into magnetic mineralogy and grain size. Measurements of temperature-dependent susceptibility (κ-T curves) were obtained using AGICO KLY-4S Kappabridge. The samples were heated (from 40 to 700 °C) and cooled back (to room temperature) in an argon atmosphere to reduce the formation of secondary magnetite or hematite. Low temperature (from about −196 °C to room temperature) κ-T curves for two samples from representative dykes were also obtained using a CS3-L apparatus coupled to the KLY-4S bridge instrument. Hysteresis measurements were carried out using a MicroMag Alternating Gradient Magnetometer (AGM) and Molspin Nuvo vibrating sample magnetometer in field of ± 1 T. Values of saturation magnetization (M_s), saturation remanent magnetization (M_{rs}), coercive force (H_c) and the coercivity of remanence (H_{cr}) were calculated from the hysteresis loops. All laboratory measurements were carried out at the Indian Institute of Geomagnetism (IIG), Navi Mumbai.

Results

Anisotropy of magnetic susceptibility (AMS)

Anisotropy of magnetic susceptibility (AMS) measurements were carried out on 349 specimens from the samples of 33 dykes selecting not less than four specimens from different samples of each dyke. These measurements were made on the fresh specimens. The AMS data for the dykes is presented in the Table 2. The mean magnetic susceptibility $(K_m) = (K_1 + K_2 + K_3)/3$ in SI units, is overall high and values range between 1.09×10^{-2} and 11.15×10^{-2} SI for present studied dykes (Table 2; Fig. 2a). The degree of anisotropy (P), given by $P = K_1/K_3$, from 1.0 to 1.5, as anticipated for basaltic rocks and values range between 1.0 and 1.3 (Fig. 2b) with an average value of 1.10 (Table 2). For the dykes with different fabric types, there is no clear relationship between P and K_m parameters (Fig. 2c). Figure 2d shows the P versus T graph (Jelinek 1981), T is expressed by $T = (\ln F - \ln L)/(\ln L - \ln F)$ where $F = K_2/K_3$ and $L = K_1/K_2$. The oblate ($T > 0$) ellipsoid shape is more predominant in the dykes even though a subordinate group is plotted in the prolate ($T < 0$) field (Fig. 2d).

The distribution of maximum, intermediate, and minimum susceptibilities at each site-dyke are plotted in Figs. 3–5. The strike of the dyke at each site is indicated for comparison with the anisotropy data. The effect of the dip on the characteristics of the magnetic fabric is insignificant. AMS data from these dykes have been grouped into three

Table 2 Anisotropy of magnetic susceptibility data for the studied dykes

Dyke	N	AMS parameters			K_1		K_2		K_3		Types of fabric
		K_m (10^{-2})	P	T	Dec	Inc	Dec	Inc	Dec	Inc	
BLI1	11	6.721	1.035	0.471	168	32	167	58	166	1	Nor
BLI2	10	4.344	1.054	−0.159	173	11	75	36	279	51	Nor
CPE1	11	1.924	1.045	−0.027	63	72	227	6	252	16	Nor
CPE2	12	2.011	1.043	−0.168	42	73	167	10	260	13	Nor
KLI1	7	4.252	1.015	0.289	104	39	220	18	159	42	Nor
MRD1	15	10.207	1.083	−0.360	83	10	217	66	223	19	Nor
MRD2	12	3.946	1.281	−0.022	116	38	182	39	280	19	Nor
MRE1	10	4.728	1.026	0.529	100	65	256	19	255	12	Nor
SRA1	6	4.091	1.142	0.181	320	45	143	26	171	27	Nor
SRA2	5	3.524	1.085	0.378	173	31	265	10	166	53	Nor
NRL2	17	2.102	1.032	0.378	171	48	46	28	300	28	Nor
NRL3	11	6.335	1.021	0.177	150	27	190	48	167	20	Nor
DGA	10	4.823	1.030	0.154	287	9	138	53	243	33	Nor
BNI	7	4.840	1.020	−0.513	50	27	197	16	200	51	Nor
SDG	12	1.185	1.028	0.258	221	38	98	49	178	8	Nor
ULE	15	3.115	1.035	−0.528	190	62	155	23	229	10	Nor
KLI4	9	2.960	1.199	−0.756	46	10	138	15	276	71	Inv
NRL1	14	7.591	1.211	0.345	193	20	154	67	228	8	Inv
NRL5	15	7.739	1.151	0.333	143	15	193	25	184	55	Inv
VHR1	7	2.092	1.150	−0.214	271	1	181	16	173	74	Inv
VHR2	8	1.089	1.053	−0.195	190	44	186	40	171	15	Inv
MRE2	8	2.000	1.129	−0.274	282	7	18	33	183	56	Inv
KSD	5	1.334	1.153	−0.211	94	9	348	60	189	29	Inv
BLR	25	5.166	1.067	−0.124	142	23	243	43	157	32	Inv
KMB	7	4.054	1.084	0.160	127	47	158	41	231	6	Inv
NVI	7	4.376	1.483	0.266	94	1	199	56	2	34	Inv
PSL	14	5.401	1.118	0.122	264	5	181	59	11	30	Inv
KLI2	8	11.150	1.101	0.440	190	74	174	11	352	11	Int
KLI3	4	4.198	1.040	−0.013	35	41	230	44	211	15	Int
VHR3	7	1.874	1.049	0.120	149	44	82	34	193	17	Int
RDA	16	6.166	1.241	−0.316	132	55	217	20	201	21	Int
NRL4	16	1.721	1.037	0.128	140	9	110	27	217	59	Int
VRI	8	5.219	1.055	0.241	165	5	278	7	122	81	Int

N number of specimens measured per dyke and included in the AMS means, *K*m mean susceptibility $[K_m = (K_1 + K_2 + K_3)/3]$, in SI units, *P* mean anisotropy degree $(P = K_1/K_3)$, *T* Jelink's parameter $[T = (\ln(K_2/K_3) - \ln(K_1/K_2))/(\ln(K_1/K_2) - \ln(K_2/K_3))]$, K_1, K_2 and K_3, maximum, intermediate and minimum susceptibility intensities, respectively, *Dec* declinations, *Inc* inclinations, Types of Fabric: *Nor* normal, *Inv* inverse, *Int* intermediate

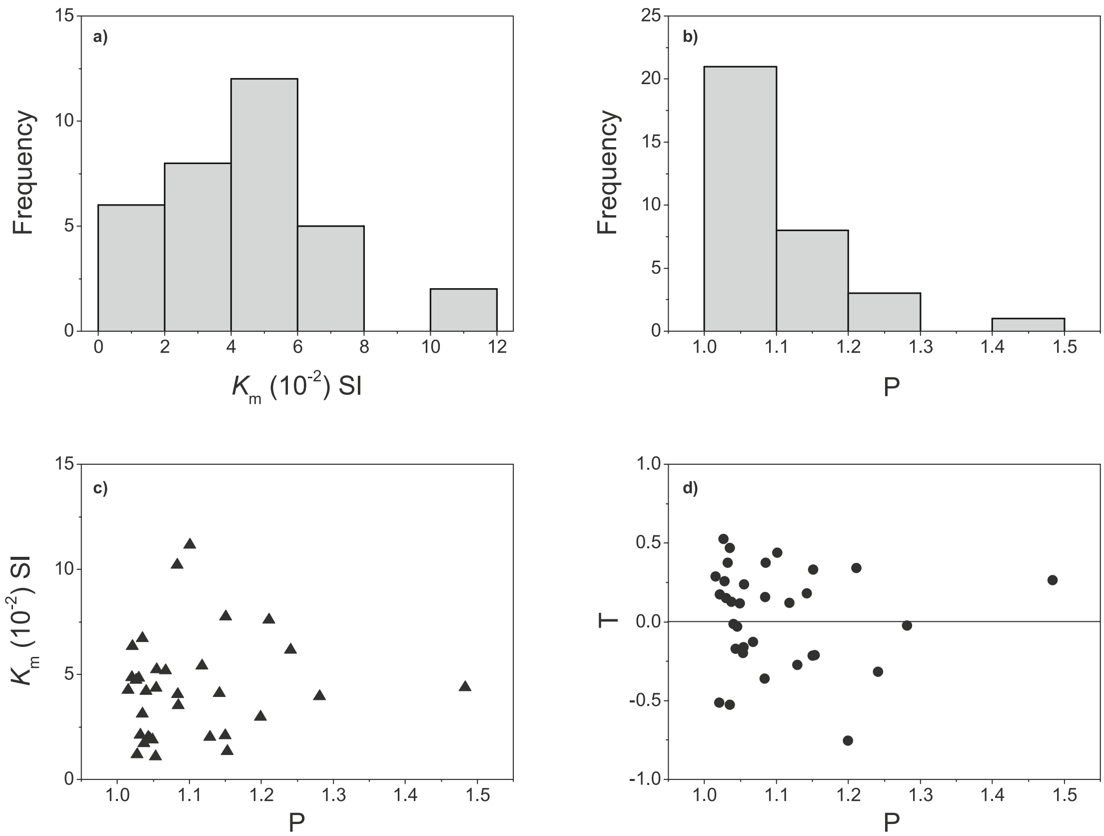

Fig. 2 **a** Histogram of the mean susceptibility *(K_m)* values; **b** Histogram of the degree of anisotropy *(P)* values; **c** *P* versus K_m and **d** *P* versus Jelinek's parameter (*T*)

(Normal, Inverse and Intermediate) categories. The first category fabric, termed as normal fabric, was characterized by the clustering of K_1 and K_2 axes on the dyke plane, whereas K_3 axes are nearly perpendicular to it (Fig. 3). Second group termed as inverse fabric in which K_2 and K_3 axes forming a plane parallel to the dyke plane and K_1 is perpendicular to that plane (Fig. 4). Third category fabric termed as Intermediate fabric, characterized by K_1 and K_3 axes clustering close to the dyke plane and the K_2 axes are perpendicular to this plane (Fig. 5).

Magnetic mineralogy

Thermomagnetic measurements (κ-T) were obtained for representative samples from dykes within the four AMS fabric types. All κ-T curves in Normal fabric, are characterized by a major decrease in magnetic susceptibility at about curie temperature (T_c) of ~ 550 °C except for KLI1 which shows decrease in susceptibility at T_c 580 °C (Fig. 6a–c). In KLI1, three variations in the slope of the heating curve 480 °C, 540 °C and 580 °C, seems to highlight the presence of either three phases of titanomagnetite or different mineralogical magnetic phases (Fig. 6a). During heating, MRD1 and MRE1 samples show two Tc points, 450 °C for MRD1 and 420 °C for MRE1 (Fig. 6a, b). The susceptibility drops at 450 °C, 420 °C and 580 °C suggests the presence of titanomagnetite and magnetite respectively. In MREI, we observe an increase in susceptibility beyond 450 °C and a rapid decrease towards 550 °C characterizing probably Hopkinson effect or Hopkinson peak. This peak highlights the presence of pure magnetite.

The susceptibility drops of the VHR2 sample, obtained from Inverse fabric, at 330–350 °C and 580 °C indicate the presence of likely Pyrrhotite (Tc~320–350 °C) and magnetite respectively (Fig. 6d). Magnetite is probably pure due to the existence of Verwey (1939) transition (around −100 °C) and the Hopkinson peak at 580 °C. The BLR sample shows three T_c at 200 °C, 390 °C and 580 °C indicating likely presence of titanomagnetite and magnetite (Fig. 6e). The KMB sample shows T_c point recorded at 580 °C indicating presence of magnetite (Fig. 6f). KMB has undergone a formation of small quantity of another phase or another magnetic mineral between 450 °C and 500 °C as seen in the slight variations in slope of the cooling and heating curves respectively. KLI2 sample from Intermediate fabric shows two Tc points recorded at 400 °C and 580 °C indicating presence

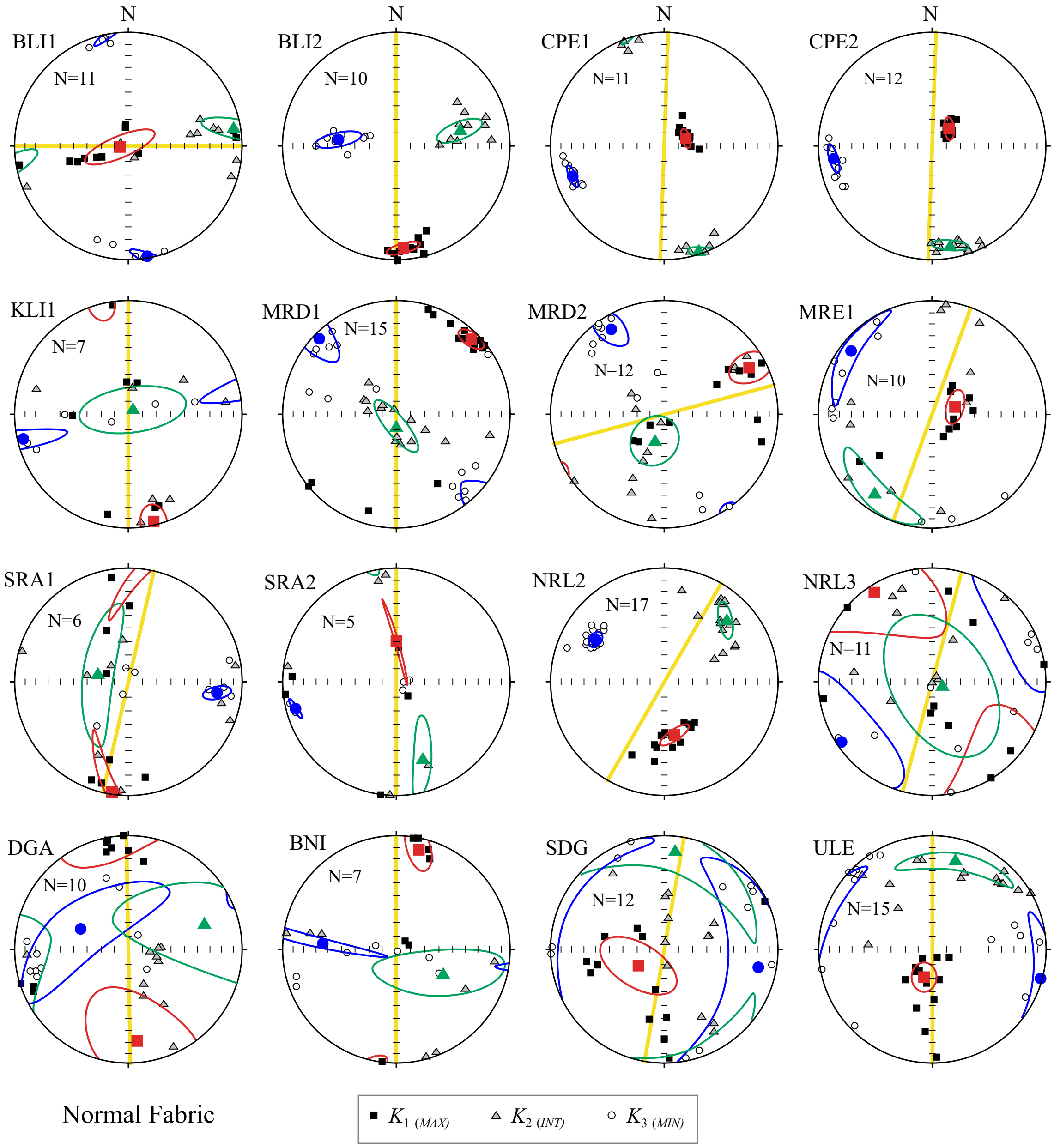

Fig. 3 Anisotropy of magnetic susceptibility data of studied dykes plotted in lower hemisphere projections for different fabrics for Normal fabric. Solid squares, triangles and open circles are maximum (K_1), Intermediate (K_2) and minimum (K_3) axes respectively. Dyke trend is shown in yellow line

of titanomagnetite and magnetite respectively (Fig. 6g). κ-T curve for the KLI3 sample show T_c at 550 °C corresponds to titanomagnetite (Fig. 6h). The heating curve for KLI3 shows two curie points, the first around 400 °C and the second around 580 °C. The cooling curve has three changes in slope towards approximately 580 °C, 510 °C and 350 °C. This supposes the formation of new magnetic phases. T_c for sample RDA of Intermediate fabric is recorded at 350 °C and 580 °C indicating presence of titanomagnetite and magnetite (Fig. 6i). In this case we have two T_c around 250 °C and 350 °C and both heating and cooling curves are reversible between 700 °C and 550 °C showing that the original amount of magnetite did not undergo mineralogical transformation (Fig. 6d, e). Heating and cooling curves of all specimen are reversible between the highest temperatures and the Curie one. This means that the original magnetite was not altered during heat treatments. The slight transformations that have occurred (reduction or oxidation) have only concerned the other existing phases. These rock magnetic analyzes highlighted the presence of titano-magnetite,

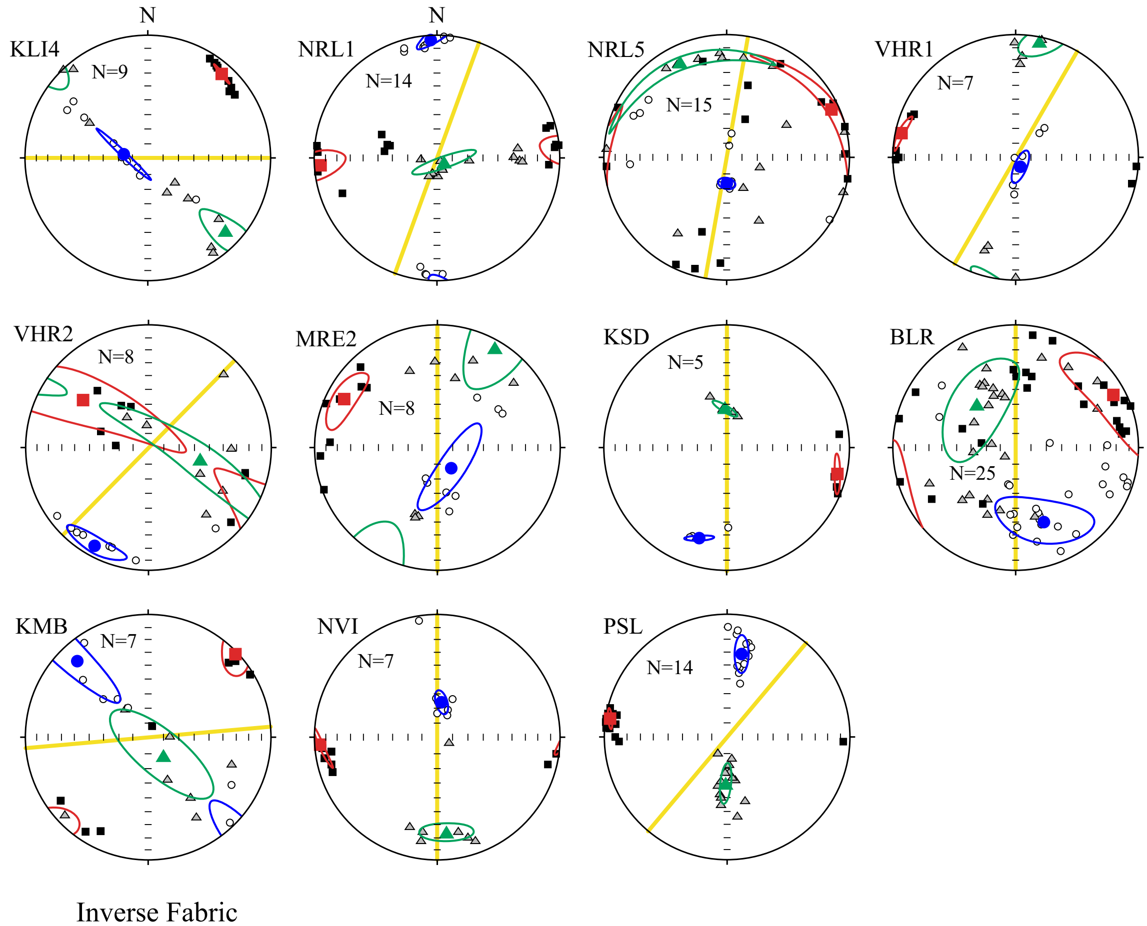

Fig. 4 Anisotropy of magnetic susceptibility data of studied dykes plotted in lower hemisphere projections for different fabrics for Inverse fabric. Solid squares, triangles and open circles are maximum *(K_1)*, Intermediate *(K_2)* and minimum *(K_3)* axes respectively. Dyke trend is shown in yellow line

magnetite, pyrrhotite and another unidentified mineral. The cooling curves showed the formation of other unidentified magnetic phases or minerals by the transformation of pre-existing minerals.

Hysteresis curves and the parameters on a Day plot (Dunlop 2002) for different fabrics from representative samples from individual dykes are shown in Fig. 7 and Table 3. Values of coercive force (H_c), saturation remanence (M_{rs}), and saturation magnetization (M_s), obtained at maximum field of 1 T were calculated after subtraction of the paramagnetic contribution. The ratio of saturation remanence to saturation magnetization (M_{rs}/M_s) and the ratio of remanence coercivity to saturation coercivity (H_{cr}/H_c) range between 0.02–0.38 and 1.32–6.25 respectively. Hysteresis curves for representative dyke samples that exhibit single domain (SD), pseudo-single domain (PSD) and multi domain (MD) behavior are shown in Fig. 7a–h. Hysteresis parameters data set in the day plot show a classic trend from PSD grains to MD grains, most probably due to a mixture of real PSD and MD grains with similar Ti substitution (Fig. 7i). The representative hysteresis loops are closed mostly around < 100 mT indicating the predominance of the ferromagnetic phases, and all the loops are saturated by 250 mT in an applied field of 1 T (Fig. 7a–h). Thinner loops (KLI1, MRD1, MRE1, BLR, KMB, KLI3 and RDA) are due to low-coercivity components while intermediate (VHR2) suggests the presence of medium coercive magnetic minerals (Fig. 7a–h).

We can thus expect for the part of the AMS carried by magnetite, with MD or Pseudo-single domain PSD, a normal magnetic fabric directly related to the shape of the magnetite grains (Potter and Stephenson 1988).

Petrographic studies have been carried out for the same 33 dykes to identify the mineral phases (Basavaiah et al. 2018 for details). Most of the samples show fine-grained basaltic composition containing phenocrysts of subhedral prismatic plagioclase and rare olivine (Fig. 8a–d). The dykes in this area are either dolerite or olivine phyric basalt, or olivine of plagioclase phyric of extremely fine-grained basalt. Dyke MRE2 show Olivine phenocrysts with alteration along margin and interstitial glass within plagioclase laths

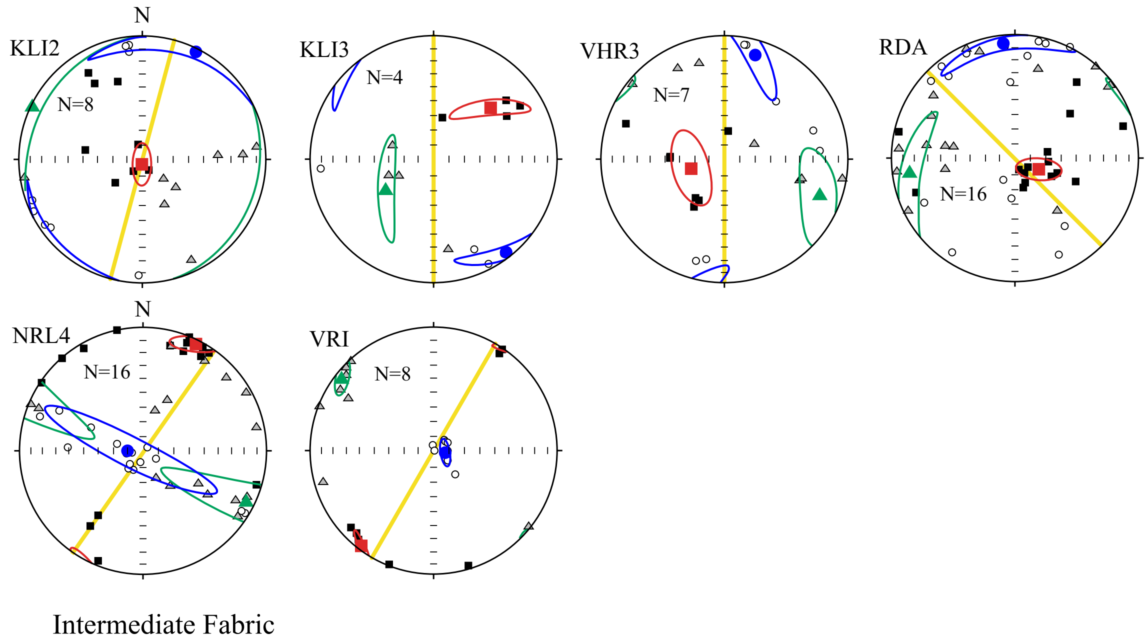

Fig. 5 Anisotropy of magnetic susceptibility data of studied dykes plotted in lower hemisphere projections for different fabrics for Intermediate fabric. Solid squares, triangles and open circles are maximum *(K_1)*, Intermediate *(K_2)* and minimum *(K_3)* axes respectively. Dyke trend is shown in yellow line

in groundmass filled with magnetite (Fig. 8a). Dyke KMB shows extremely fine grained basalt with phenocrysts of plagioclase prism and subhedral squarish opaque (Fig. 8b). Dyke MRD2 contains extremely fine grained basalt with elongated crystals of plagioclase as phenocrysts (Fig. 8c). Dyke KLI2 shows phenocrysts of elongated crystals of plagioclase in extremely fine grained basalt (Fig. 8d).

Discussions

Normal fabric was observed in 16 dykes and occurred in 48.5% of the dykes (Fig. 3). This kind of fabric was also found in earlier studies of dyke swarms (Rochette et al. 1992; Prasad et al. 1999; Raposo and D'Argella-Filho 2000; Rapaleni and Luchi 2000; Kumar et al. 2015; Ramesh et al. 2020). Normal fabric has been interpreted as a flow fabric with K_1 as the flow indicator (Knight and Walker 1988). Several investigators have used the K_1 inclination (IK_1) of normal fabric to deduce the distance between the fractures and magma source (e.g. Ernst and Baragar 1992; Raposo and Ernesto 1995; Knight and Walker 1988). In dykes with $IK_1 < 30°$ is an indication that the dykes were fed by horizontal or sub-horizontal flow (Raposo and D'Argella-Filho 2000). Five dykes appear to be fed by horizontal flow and distributed in the south of Mumbai of Wai Formation. The horizontal magma flow direction revealed by sub-horizontal inclinations in these dykes suggests that the source could be located far away. This type of flow pattern is observed in several dyke swarms (Ernst 1990; Raposo and Ernesto 1995; Hastie et al. 2014; Ramesh et al. 2020). Ray et al. (2008) also assumed about the presence of both inclined to subvertical upward and lateral (although very rare) injection in Central Deccan Traps. Delcamp et al. (2014) reported a similar flow pattern from the mafic dykes of the Tenerife NE rift zone. They compared the upward subvertical flows with the summit eruptions just above the shallow crustal chambers and inclined to distant lateral flow away at the flanks (Njome et al. 2008; Wantim et al. 2011).

The value $30° < IK_1 < 60°$ was assumed to indicate inclined flow and $IK_1 > 60°$ indicated the vertical flow. In the present study, seven dykes fed by inclined westward flows and four dykes have the steepest K_1 suggests that the region could be closer to a magma source. However, the flow distribution is random and does not show any preferred pattern to suggest the single magma chamber from deep-seated source. In this scenario, the possible interpretation could be the presence of multiple subsurface magma chambers which are responsible for the random distribution. AMS analysis by Das et al. (2021) suggests that the Dhule-Nandurbar Deccan dyke swarm display dominantly subvertical to inclined flow and occasional sub-horizontal/lateral flow. Their study also suggests the presence of multiple sub-surface magma centres from which magma pulses got injected through crustal fissures.

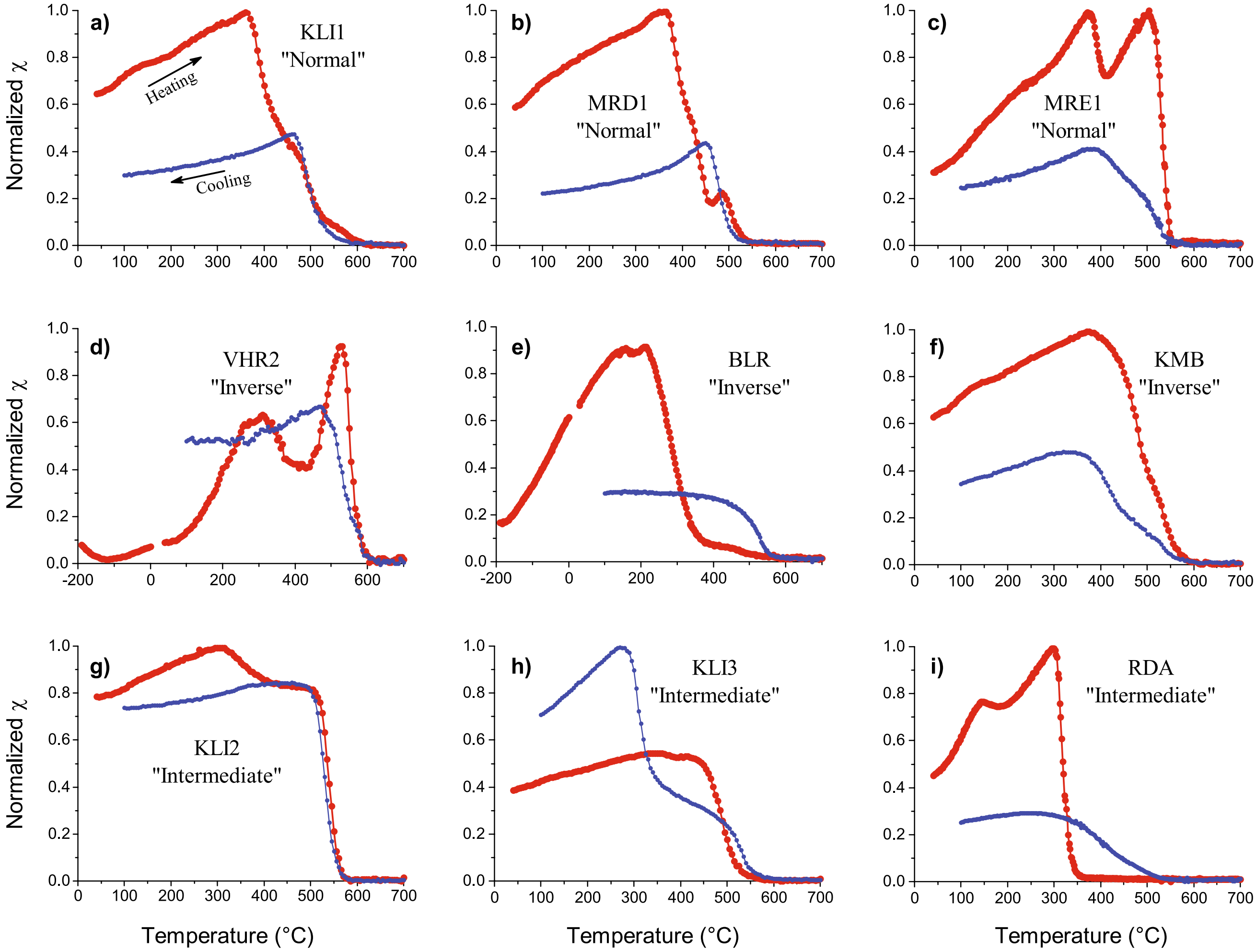

Fig. 6 Representative magnetic susceptibility versus temperature (Low and high) curves for samples with different AMS fabrics **a-c** normal fabric; **d-f** inverse fabric and **g-i** intermediate. The red and blue lines are heating and cooling cycles respectively

Based on isotopic and geochemical characteristics, Vanderkluysen et al. (2011) and Hooper et al. (2010) inferred that the N–S dykes in the coastal area were a product of post-Deccan Seychelles rifting following the main phase of volcanism, and that the dykes with no preferred orientation in the coastal area were most likely feeders for the three main upper Formations (Fms) of the Wai subgroup (Poladpur, Ambenali and Mahabaleshwar). Moreover, Vanderkluysen et al. (2011) identified the dyke swarm as likely feeders for the lower and middle Fms (Fig. 1b) exhibiting preferred orientations consistent with the rifting based model, whereas the dyke swarms with no preferred orientation inferred to be the feeder dykes of the top Fms are inconsistent with the rifting model. Geophysical model by Bhattacharji et al (2004) reported that the mafic bodies appearing as magma chambers along the western continental margin rift in the upper lithosphere. They are considered as the major reservoirs for the Deccan flood basalt volcanism. Petrological modeling based on olivine clinopyroxene- plagioclase saturated liquid compositions (Grove et al. 1992), using geochemical data on feeder dikes and lowermost Deccan lava flows in the Narmada-Tapti valley and near Surat, also indicates that the Deccan magmas last equilibrated in feeder dikes and associated underlying multiple magma chambers at a depth of about 7 km along the Narmada-Tapti and western continental margin rifts (Bhattacharji et al 1996). $^{40}Ar/^{39}Ar$ and K–Ar age dating of the feeder dikes and associated lower Deccan lavas indicate that they were coeval and erupted at approximately 65 Ma (Bhattacharji et al 1996). Although no direct physical field evidence of a feeder dyke is found, geophysical, geochemical, and AMS data indirectly proves that the dyke swarm was most likely a feeder dyke swarm to some part of the Deccan flood basalt. Geochemical, petrological and geophysical studies infer the presence of multiple magma chambers at shallow crustal surface (Bhattacharji et al. 1996), which supports flow. The paleomagnetic study carried out by Basavaiah et al. (2018), highlights successive flows at different periods (~65 and ~80 Ma) with Normal

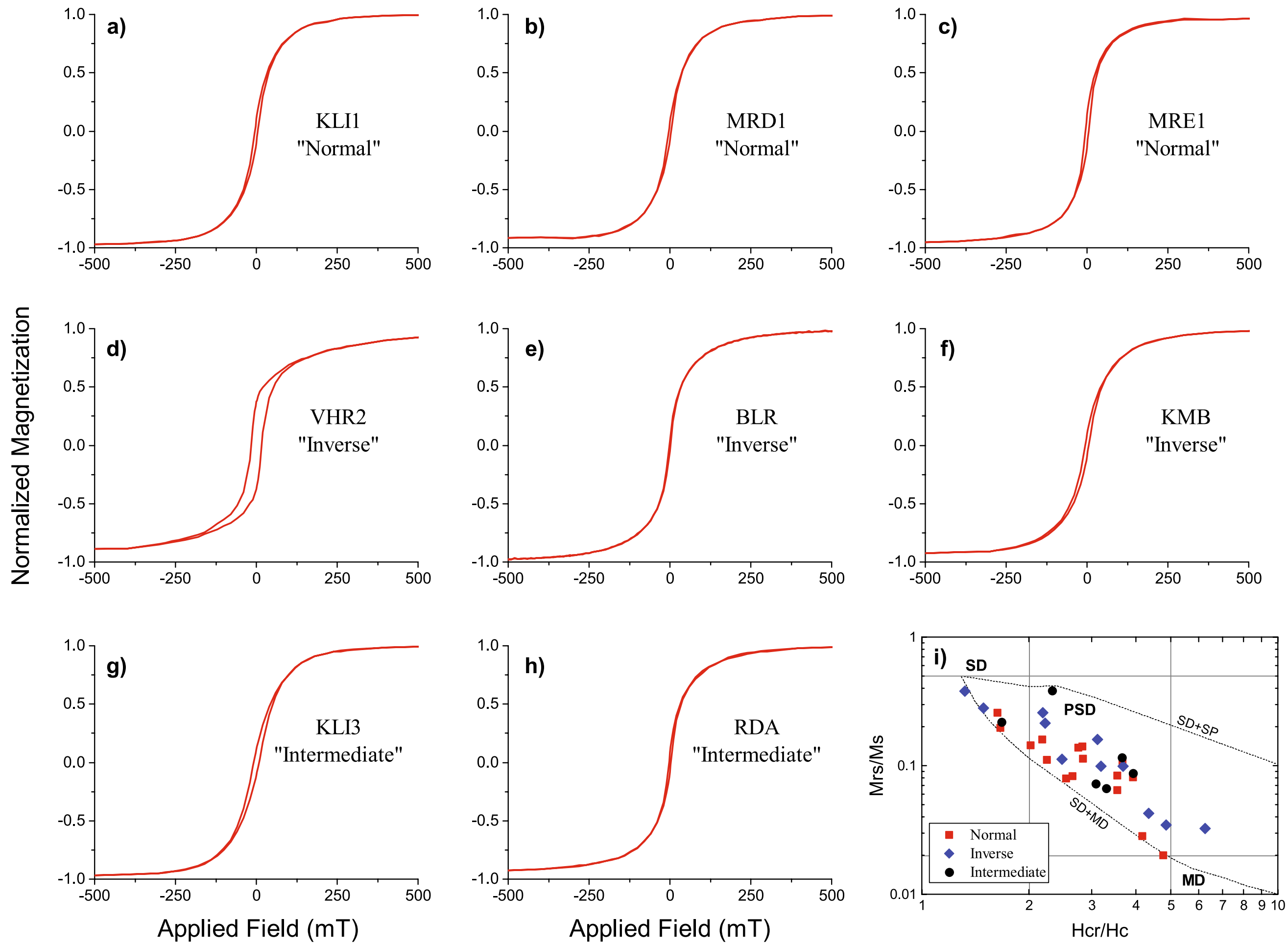

Fig. 7 Representative hysteresis loops for the studied dykes **a-c** normal fabric, **d-f** inverse fabric **g**, **h** intermediate fabric and **i** hysteresis parameter ratios of M_{rs}/M_s versus H_{cr}/H_c for samples from the west coast dykes, Mumbai (after Day et al. 1977) with the boundaries of SD and MD behaviour for magnetite taken from the values of Dunlop (2002). M_{rs} saturation remanence, M_s saturation magnetization, H_{cr} remanence coercivity, H_c coercive force. Hysteresis measurement cycles were performed for ± 1 T and in the figure, plotted only for ± 0.5 T for a better view

and Reverse polarities. The results show that between these two periods India drifted about 4.4° in altitude. This may indicate that the sources emitting magma are different. In addition, the fact that the dykes have been tilted, the horizontal and vertical distances of the magma emitting sources relative to the outcrop also vary likely.The random distribution of magma in the present study is thus consistent with these conclusions.

The inverse fabric has been observed in ten dykes and occurred in 33% of the dykes (Fig. 4). The inverse fabric in dykes has been interpreted to be due to secondary processes such as post-emplacement modification, hydrothermal alteration, or due to the presence of SD particles in the rocks (Rochette et al. 1992). The hysteresis parameters in the Day plot shows that all the samples fall into the PSD to MD range (Fig. 7i) and are found in other dyke swarms (Tauxe et al. 1998; Raposo and Ernesto 1995). As petrographic analyses showed no evidence either of later alteration due to hydrothermaluids and either metamorphism or solid-state deformation. Alternatively, this Inverse fabric could be related to local irregularities that occurred after dyke emplacement. As seen in Fig. 4, clusters of K_2 and K_3 in the case of two dykes (KMB and KLI4) are disposed symmetrically on the opposite sides of the dyke trend with an offset of about 30° from the trend. The K_1 cluster also is displaced by the same amount from the perpendicularity of the dyke trend. The remaining dykes appear to meet the requirement of this fabric nearly well.

Intermediate fabric, which is characterized by clustering of K_1 and K_3 axes close to the dyke orientation plane and K_2 axes are perpendicular to it (Fig. 5) and is very nearly exhibited by only six dykes. This fabric occurs in 18.2% of the dykes. This kind of fabric was also found in earlier studies of dyke swarms (Rochette et al. 1992;

Table 3 Summary of hysteresis measurements of studied dykes

Dyke	χlow $\times10^{-10}m^3kg^{-1}$	χhigh $\times10^{-10}m^3kg^{-1}$	χferri $\times10^{-10}m^3kg^{-1}$	χferri%	χhigh%	$M_s\times10^{-3}$ Am^2kg^{-1}	$M_{rs}\times10^{-3}$ Am^2kg^{-1}	H_c (mT)	H_{cr} (mT)
BLI1	225.1	1.0	224.1	99.6	0.4	945.6	79.0	4.4	15.7
BLI2	251.8	3.0	248.8	98.8	1.2	778.3	50.2	2.3	8.1
CPE1	125.8	3.1	122.7	97.6	2.4	679.2	75.5	6.6	14.8
CPE2	195.1	3.4	191.6	98.2	1.8	1011.0	80.6	4.6	11.6
KLI1	498.1	2.5	495.6	99.5	0.5	1760.0	185.0	4.4	16.3
MRD1	180.8	0.7	180.2	99.6	0.4	700.8	57.0	3.3	13.1
MRD2	137.9	0.8	137.1	99.4	0.6	513.7	71.0	6.1	16.8
MRE1	463.2	1.7	461.5	99.6	0.4	1331.0	188.1	5.0	14.1
SRA1	98.3	1.0	97.3	99.0	1.0	371.3	59.3	7.2	15.7
SRA2	210.5	3.3	207.3	98.4	1.6	1265.0	25.4	1.5	7.2
NRL2	157.5	2.9	154.6	98.2	1.8	1120.0	290.0	19.4	31.6
NRL3	243.8	1.6	242.2	99.3	0.7	1837.0	51.9	2.7	11.2
DGA	335.2	2.2	333.0	99.4	0.6	1432.0	119.1	4.0	10.7
BNI	602.2	0.5	601.7	99.9	0.1	3999.0	455.4	8.7	24.7
SDG	46.8	2.0	44.8	95.7	4.3	240.7	34.8	8.7	17.6
ULE	330.4	4.1	326.3	98.8	1.2	2452.0	483.2	15.5	25.7
KLI4	174.5	2.3	172.2	98.7	1.3	305.6	49.1	3.3	10.4
NRL1	480.2	3.1	477.1	99.4	0.6	1183.0	41.0	1.0	4.8
NRL5	576.5	3.5	573.0	99.4	0.6	1361.0	44.4	0.9	5.7
VHR1	8.1	0.3	7.8	96.6	3.4	29.6	8.3	10.6	15.7
VHR2	24.4	2.3	22.2	90.8	9.2	199.2	75.9	15.6	20.5
MRE2	192.3	2.4	189.9	98.7	1.3	377.9	80.9	4.4	9.9
KSD	59.8	1.1	58.7	98.1	1.9	183.2	47.2	8.9	19.5
BLR	102.3	2.8	99.5	97.3	2.7	346.4	14.8	1.7	7.4
KMB	44.4	1.0	43.4	97.7	2.3	185.6	18.4	5.0	18.4
NVI	61.5	0.5	61.1	99.2	0.8	132.0	13.1	2.8	8.8
PSL	144.3	4.3	139.9	97.0	3.0	1093.0	122.6	4.0	9.9
KLI2	36.1	0.2	35.9	99.5	0.5	230.3	15.3	5.6	18.4
KLI3	249.2	2.8	246.4	98.9	1.1	1404.9	162.6	7.8	28.5
VHR3	135.5	3.4	132.1	97.5	2.5	409.3	157.0	12.2	28.5
RDA	611.7	0.7	611.0	99.9	0.1	1755.9	153.9	2.8	10.9
NRL4	145.2	2.3	142.9	98.4	1.6	691.2	151.4	10.5	17.6
VRI	248.2	3.9	244.4	98.4	1.6	1571.0	114.0	2.6	7.9

χlow low field susceptibility, *χhigh* high field susceptibility, *χferri* difference between χlow and χhigh, *χferri%* percentage of ferromagnetic contribution, *χhigh%* percentage held in paramagnetic and high coercive antiferromagnetic phases, M_s saturation magnetization, M_{rs} saturation remanent magnetization, H_c coercivity, and H_{cr} coercivity of remanence

Raposo and D'Argella-Filho 2000; Rapaleni and Luchi 2000). The intermediate fabric has been interpreted to be due to the presence of fine-grained, particularly PSD grains (Rochette et al. 1992; Aubourg et al. 1995). This interpretation cannot be applied to fabric found in present study dykes, since all the three normal, inverse and intermediate fabric samples fall in-to PSD/MD range (Fig. 7i). In the present study, the intermediate fabric in the dykes might be caused due to the vertical compaction of a static magma column with minimum stress along the dyke direction (Park et al. 1988; Raposo and D'Argella-Filho 2000).

Conclusions

The following conclusions can be drawn from the AMS study of 33 dykes from West coast of Maharashtra, DVP:

(1) The magnetic mineralogy studies indicate the probable presence of a complex combination of ferrimagnetic grains in the size range PSD/MD. Out of 33 dykes, 27 dykes are dominated by PSD, five are in SD and one in MD.

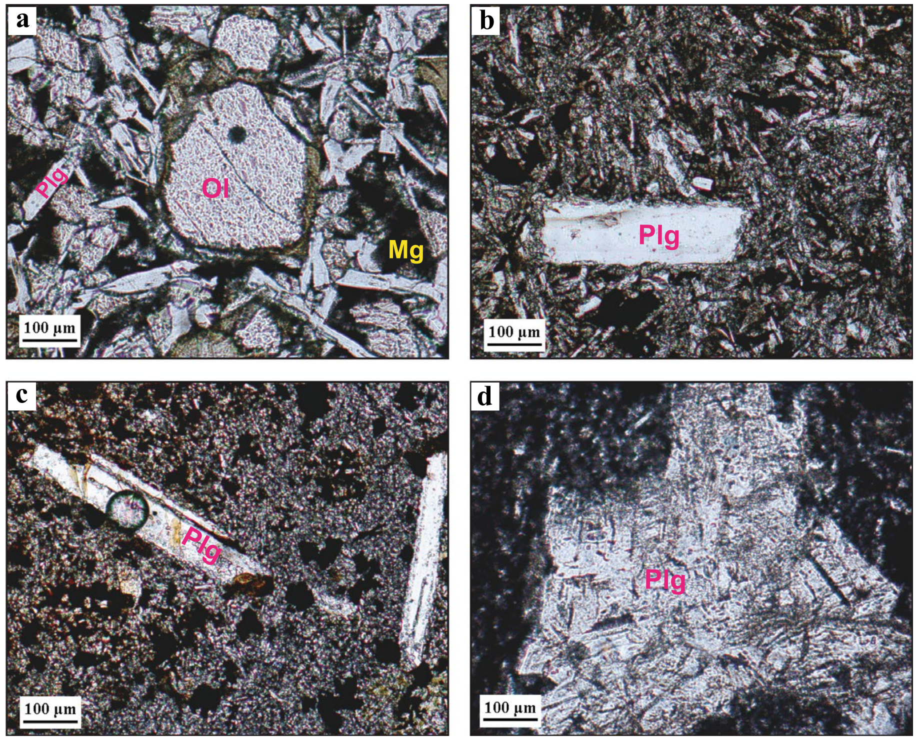

Fig. 8 Representative Thin section images for the studied dykes. **a** MRE2: Olivine phenocrysts with alteration along margin and interstitial glass within plagioclase laths in groundmass filled with magnetite. **b** KMB: Extremely fine grained basalt with phenocrysts of plagioclase prism and subhedral squarish opaque. **c** MRD2: Extremely fine grained basalt with elongated crystals of plagioclase as phenocrysts and **d** KLI2: Phenocrysts of elongated crystals of plagioclase in extremely fine grained basalt. Legend for mineral recognition: Plagioclase (Plg), Olivine (Ol) and Magnetite (Mg). See the text for further explanation

(2) The AMS study has yielded three kinds of magnetic fabric: normal, inverse, and intermediate based on the clustering of K_1, K_2 and K_3 axes with respect to the dyke planes.
(3) Normal fabric displays clustering of K_1–K_2 axes in the dyke plane and K_3 axes are normal to the dyke plane. This fabric could reflect the magma flow. Intermediate fabric found in six dykes and was characterized by K_1–K_3 axes clusters close to dyke plane whereas K_2 axes are perpendicular to the dyke plane. Inverse fabric defined by K_2–K_3 plane parallel to the dyke plane and K_1 perpendicular to dyke plane, found in 11 dykes.
(4) The inclination of IK_1 axes, which gives magma flow direction in dykes displaying normal fabric, dykes were mainly fed by inclined westward plunging flows ($30° < IK_1 < 60°$) to the steepest IK_1 ($> 60°$) suggests that the dykes may be closer to magma source. Horizontal magma flow inferred from three dykes reveals source is located further away.
(5) Presence of multiple trends of primary flow axes revealed from AMS study support subsurface magma chambers which are responsible for the random distribution. Subvertical upward flow indicates the proximity of source chamber. The observed flow from the present study together with geophysical, geochemical and petrological evidences provided by previous studies support indirect evidences of the theory of fissure fed volcanism.

Acknowledgements We are most grateful to Editor and four anonymous reviewers for encouraging comments and suggestions which have helped in vastly improving the manuscript. Authors thank Mr. Varun Dongre for his continuous support of laboratory instrument maintenance.

Author contributions B.V. Lakshmi contributed to the study conception and design. Material preparation, data collection and analysis were performed by both B.V. Lakshmi and K. Deenadayalan, discussions and final review by A.P. Dimri. The first draft of the manuscript was written by B.V. Lakshmi and all the three authors read and approved the final manuscript.

Funding This work was supported by DST-IIG fund.

Data availability Data supporting this study are available from the Corresponding Author on request.

Declarations

Conflict of interest The authors declare no competing interests.

References

Aubourg C, Rochette P, Berguller F (1995) Composite magnetic fabric in weakly deformed black shales. Phys Earth Planet Inter 87:267–278

Basavaiah N, Satyanarayana KVV, Deenadayalan K, Prasad JN (2018) Does Deccan volcanic sequence contain more reversals than the three-Chron N-R–N flow magnetostratigraphy?—A palaeomagnetic evidence from the dyke-swarm near Mumbai. Geophys J Int 213:1503–1523

Bean JE, Turner CA, Hooper PR, Subbarao KV, Walsh JN (1986) Stratrigraphy, composition and formation of Deccan basalts, Western ghats. India Bull Volcanol 48:61–83
Bhattacharji S, Chatterjee N, Wampler JM, Nayak PN, Deshmukh SS (1996) Indian intraplate and continental margin rifting, lithospheric extension, and mantle upwelling in Deccan flood Basalt volcanism near the K/T boundary: evidence from mafic dike swarms. J Geol 104:379–398
Bhattacharji S, Sharma R, Chatterjee N (2004) Two and three dimensional modelling along western continental margin and intraplate Narmada-Tapti rifts: its relevance to Deccan flood basalt volcanism. J Earth Syst Sci 113:771–784
Bondre NR, Hart WK, Sheth HC (2006) Geology and geochemistry of the Sangamner mafic dyke swarm, western Deccan volcanic province, India: implications for regional stratigraphy. J Geol 114:155–170
Borradaile GJ, Jackson M (2004) Anisotropy of magnetic susceptibility (AMS): magnetic petrofabrics of deformed rocks. Geol Soc Lond Spec Publ 238:299–360
Bradak B, Kovacs J, Magyari A (2019) The origin and significance of some 'irregular' loess magnetic fabric found in the Paks succession (Hungary). Geophys J Int 217:1742–1754
Campbell IH, Griffiths RW (1990) Implications of mantle plume structure for the evolution of flood basalts. Earth Planet Sci Lett 99:79–93
Canon-Tapia E, Herrero-Bervera E (2009) Sampling strategies and the anisotropy of magnetic susceptibility of dykes. Tectonophysics 466:3–17
Chadima M, Jelinek V (2009) Anisoft 4.2: anisotropy data browser. Contrib Geophys Geod 38:38
Chao H, Son M, Sohn YK, Park ME (2017) Magnetic fabric (anisotropy of magnetic susceptibility) constraints on emplacement mechanism of clastic dikes. J Geophys Res Solid Earth 122:3306–3333. https://doi.org/10.1002/2016JB013583
Chenet AL, Fluteau F, Courtillot V, Gerard M, Subbarao KV (2008) Determination of rapid Deccan eruptions across the cretaceous-tertiary boundary using paleomagnetic secular variation: results from a 1200-m-thick section in the Mahabaleshwar. J Geophys Res 113:B04101. https://doi.org/10.1029/2006JB004635
Courtillot V, Gallet Y, Rocchia R, Feraud G, Robin E, Hoffman C, Bhandari N, Ghevariya ZG (2000) Cosmic markers, 40Ar/39Ar dating and paleomagentism of the KT sections in the Anjar area of the Deccan large igneous province. Earth Planet Sci Lett 182:137–156
Courtillot V, Renne PR (2003) On the ages of flood basalt events. Comp Rend Geosci 335:113–140
Curtis ML, Riley TR, Owens WH, Leat PT, Duncan RA (2008) The form, distribution and anisotropy of magnetic susceptibility of Jurassic dykes in H.U. Sverdrupfjella, Dronning Maud land, Antarctica. Implications for dyke swarm emplacement. J Struct Geol 30:1429–1447
Das A, Mallik J, Banerjee S (2021) Characterization of the magma flow direction in the Nandurbar-Dhule Deccan dyke swarm inferred from magnetic fabric analysis. Phys Earth Planet Inter 319:106782
Day R, Fuller MD, Schmidt VA (1977) Hysteresis properties of titanomagnetites: grain size and composition dependence. Phys Earth Planet Inter 13:260–266
Delcamp A, Petronis MS, Troll VR (2014) Discerning magmatic flow patterns in shallow-level basaltic dykes from the NE rift zone of Tenerife, Spain, using the anisotropy of magnetic susceptibility (AMS) technique. Geol Soc Lond Spec Publ 396:87–106
Deshmukh SS, Sehgal MN (1988) Mafic dyke swarms in Deccan volcanic province of Madhya Pradesh and Maharashtra. Geol Soc India Mem 10:323–340
Dessai AG, Viegas A (1995) Multi-generation mafic dyke swarm related to Deccan magmatism, south of Bombay: implications on the evolution of the western Indian continental margin, in dyke swarms of peninsular India. Geol Soc India Mem 33:435–451
Dessai AG, Bertrand H (1995) The "Panvel Flexure" along the western Indian continental margin: an extensional fault structure related to Deccan magmatism. Tectonophysics 241(1–2):165–178
Dunlop DJ (2002) Theory and application of Day plot (Mrs/Ms versus Hcr/Hc) 2. Application to data for rocks, sediments, and soils. J Geophys Res 107:2057
Ernst RE (1990) Magma flow in two mafic Proterozoic dyke swarms of the Canadian shield as estimated using anisotropy of magnetic susceptibility data. In: Paker AJ, Rickwood PC, Tucker DH (eds) Mafic dykes and emplacement mechanisms. AA Balkema, Rotterdam, pp 231–235
Ernst RE, Baragar WRA (1992) Evidence from magnetic fabric to the flow pattern of magma in the Mackenzie giant radiating dyke swarm. Nature 356:511–513
Font E, Nascimento C, Omira R, Baptista MA, Silva PF (2010) Identification of tsunami-induced deposits using numerical modeling and rock magnetism techniques: a study case of the 1755 Lisbon tsunami in Algarve. Portugal Phys Earth Planet Inter 182:187–198
Grove TL, Kinzler RJ, Bryan WB (1992) Fractionation of mid-ocean ridge basalt (MORB). Mantle Flow and Melt Generation at Mid-Ocean Ridges. Geophysical Monograph 71:281–310
Hastie WW, Watkeys MK, Aubourg C (2014) Magma flow in dyke swarms ofthe Karoo LIP: implications for the mantle plume hypothesis. Gondwana Res 25:736–755
Hooper P, Widdowson M, Simon K (2010) Tectonic setting and timing of the final Deccan flood basalt eruptions. Geology 39(9):839–842
Hrouda F (1982) Magnetic anisotropy of rocks and its applications in geology and geophysics. Geophys Suru 5:37–82
Jelinek V (1981) Characterization of the magnetic fabric of rocks. Tectonophysics 79(3–4):63–67
Khan AM (1962) The anisotropy of magnetic susceptibility of some igneous and metamorphic rocks. J Geophys Res 67:2873–2885
Knight MD, Walker GPL (1988) Magma flow directions in dykes of the Koolau complex Oahu, determined from magnetic fabric studies. J Geophys Res 93:4301–4319
Kumar A, Parashuramulu V, Nagaraju E (2015) A 2082 Ma radiating dyke swarm in the eastern Dharwar craton, southern India and its implications to Cuddapah basin formation. Precamb Res 266:490–505
Lakshmi BV, Satyanarayana KVV, Basavaiah N, Gawali PB (2015) Anisotropy of magnetic susceptibility of earthquake-affected soft sediments: example from Ther village, Latur, Maharashtra. India Curr Sci 108(4):708–712
Lakshmi BV, Deenadayalan K, Gawali PB, Misra S (2020) Effects of Killari earthquake on the paleo-channel of Tirna river basin from central India using anisotropy of magnetic susceptibility. Sci Rep 10(1):1–12
Levi T, Weinberger R, Aı¨fa T, Eyal Y, Marco S, (2006) Injection mechanism of clay-rich sediments into dikes during earthquakes. Geochem Geophys Geosyst 7:Q12009
Levi T, Weinberger R, Marco S (2014) Magnetic fabrics induced by dynamic faulting reveal damage zone sizes in soft rocks, Dead sea basin. Geophys J Int 199:1214–1229
Maffione M, Hernandez-Moreno C, Ghiglione MC, Speranza F, van Hinsbergen DJ, Lodolo E (2015) Constraints on deformation of the southern Andes since the cretaceous from anisotropy of magnetic susceptibility. Tectonophysics 665:236–250
Mahoney JJ (1988) Deccan traps. In: MacDougall JD (ed) Continental flood basalts. Kluwer, Dordrecht, pp 151–194
Mallik J, Mathew G, Greiling R (2009) Magnetic fabric variations along the fault related anticlines of eastern Kachchh, western India. Tectonophysics 473:428–445
Mamtani MA, Pal T, Greiling RO (2013) Kinematic analysis using AMS data from a deformed granitoid. J Struct Geol 50:119–132

Morgan WJ (1981) Hotspot tracks and the opening of the Atlantic and Indian ocean. In: Emiliani C (ed) The sea. Wiley, New York
Morner NA, Sun G (2008) Paleoearthquake deformations recorded by magnetic variables. Earth Planet Sci Lett 267:495–502
Nagaraju J, Chetty T, Prasad GV, Patil S (2008) Transpressional tectonics during the emplacement of Pasupugallu Gabbro Pluton, western margin of Eastern ghats mobile belt, India: evidence from AMS fabrics. Precamb Res 162:86–101
Njome SM, Suh CE, Sparks RJ, Ayonghe SN, Fitton JG (2008) The mount Cameroon 1959 compound lava flow field: morphology, petrology and geochemistry. Swiss J Geosci 101:85–98
Pan X, Shen Z, Roberts PA, Heslop D, Shi L (2014) Syntectonic emplacement of late cretaceous mafic dyke swarms in coastal southeastern China: insights from magnetic fabrics, rock magnetism and field evidence. Tectonophysics 637:328–340
Parés JM, van der Pluijm BA, Dinarès-Turell J (1999) Evolution of magnetic fabrics during incipient deformation of mudrocks (Pyrenees, northern Spain). Tectonophysics 307:1–14
Park K, Tanczyk EI, Desbarats A (1988) Magnetic fabric and its significance in the 1400 Ma Mealy diabase dykes of Labrador. Can J Geophys Res 93:13689–13704
Pascoe EH (1964) A manual of geology of India and Burma. Gov India Publ New Delhi 3:1345–2130
Patil SK, Arora BR (2003) Paleomagnetic studies on the dykes of Mumbai region, west coast of Deccan volcanic province: implications on age and span of the Deccan eruptions. J Virtual Explo 12:107–116
Potter D, Stephenson A (1988) Single-domain particles in rocks and magnetic fabric analysis. Geophys Res Lett 15:1097–1100
Powar KB, Vadetwar SV (1995) Mineralogy and geochemistry of basic dykes and associated plugs of the Revas-Murud sector, Konkan coastal belt. Maharashtra Geol Soc India Mem 33:339–363
Prasad JN, Patil SK, Saraf PD, Venkateshwarlu M, Rao DRK (1996) Paleomagnetism of dyke swarm from the Deccan volcanic province of India. J Geomagn Geoelectr 48:977–991
Prasad JN, Satyanarayana KVV, Gawali PB (1999) Palaeomagnetic and low-field AMS studies of Proterozoic dykes and their basement rocks around Harohalli. South India J Geol Soc India 54:57–68
Pratheesh P, Prasannakumar V, Praveen KR (2011) Mafic dykes of Moyar shear zone, north Kerala, India: emplacement history and petrogenetic interpretation based on structure, geochemistry and magnetic fabric. Iran J Earth Sci 3:185–193
Radhakrishna T, Joseph M (1993) Proterozoic palaeomagnetism of south Indian shield and tectonic constraints. Geol Soc India Mem 25:321–336
Ramesh BN, Nagaraju E, Parashuramulu V, Venkateshwarlu M (2020) Preliminary anisotropy of magnetic susceptibility studies on 2367 Ma Bangalore-Karimnagar giant dyke swarm, southern India: implications for magma flow. Phys Earth Planet Inter 306:106540
Rao JM (2002) Petrology and geochemistry of Dolerite dykes, west Garo hills, Meghalaya: a preliminary study. Gondwana Res 5:884–888
Rapalini AE, de Luchi ML (2000) Paleomagnetism and magnetic fabric of Midle Jurassic dykes from Western Patagonia. Argentina Phys Earth Plant Inter 120:11–27
Raposo MIB, D'Argella-Filho MS (2000) Magnetic fabrics of dyke swarms from SE Bahia state, Brazil:their significance and implications for Mesoproterozoic basic magmatism in the São Fancisco Craton. Precamb Res 99:309–325
Raposo MIB, Ernesto M (1995) Anisotropy of magnetic susceptibility in the Ponta Grossa dyke swarm (Brazil) and its relationship with magma flow directions. Phys Earth Planet Inter 87:183–196
Raposo MIB, Chaves AO, Lojkasek-Lima P, D'Agrella-Filho MS, Teixeira W (2004) Magnetic fabrics and rock magnetism of Proterozoic dike swarm from the southern São Francisco Craton, Minas Gerais state, Brazil. Tectonophysics 378:43–63
Ray R, Sheth HC, Mallik J (2007) Structure and emplacement of the Nandurbar-Dhule mafic dyke swarm, Deccan traps, and the tectonomagmatic evolution of flood basalts. Bull Volcanol 69:537
Ray R, Shukla AD, Sheth HC, Ray JS, Duraiswami RA, Vanderkluysen L, Rautela CS, Mallik J (2008) Highly heterogenous Precambrian basement under the central Deccan traps: direct evidence from xenoliths in dykes. Gondwana Res 13:375–385
Renjith A, Mamtani MA, Urai JL (2016) Fabric analysis of quartzites with negative magnetic susceptibility–does AMS provide information of SPO or CPO of quartz? J Struct Geol 82:48–59
Richards MA, Duncan RA, Courtillot VE (1989) Flood basalts and hotspot tracks: plume heads and tails. Science 246:103–107
Rochette P, Jackson M, Aubourg C (1992) Rock magnetism and the interpretation of anisotropy magnetic susceptibility. Rev Geophys 30:209–226
Sheth HC (1999) A historical approach to continental flood basalt volcanism: insights into pre-volcanic rifting, sedimentation, and early alkaline magmatism. Earth Planet Sci Lett 168:19–26
Sheth HC (2000) The timing of crustal extension, dyking, and the eruption of the Deccan flood basalts. Int Geol Rev 42:1007–1016
Sheth HC (2005) From Deccan to reunion: no trace of a mantle plume. Spec Pap Geol Soc Am 388:477–501
Srivastava RK (2006) Geochemistry and petrogenesis of neoarchaean high-Mg low-Ti mafic igneous rocks in an intracratonic setting, central India craton: evidence for boninite magmatism. Geochem J 40:15–31
Subbarao KV, Ramasubba Reddy N, Prasad CVRK (1988) Geochemistry and paleomagnetism of dykes from Mandaleshwar region. Deccan basalt province. Geol Soc India Mem 10:225–233
Subbarao KV, Hooper PR (1988) Reconnaisance map of the Deccan basalt group in the western Ghats, India. In: Subbararo KV (ed) Deccan flood basalts. Geol. Soc. India Mem., Bangalore
Tarling DH, Hrouda F (1993) The magnetic anisotropy of rocks. Chapman & Hall, London and New York, p 247
Tauxe L, Gee J, Staudigel H (1998) Flow directions in dikes from anisotropy of magnetic susceptibility data: the bootstrap way. J Geophys Res 103:17775–17790
Vandamme D, Courtillot V, Besse J, Montigny R (1991) Paleomagnetism and age determination of the Deccan traps (India): results of a Nagpur-Bombay traverse and review of earlier work. Rev Geophys 29:159–190
Vanderkluysen L, Mahoney JJ, Hoope PR, Sheth HC, Ray R (2011) The feeder system of the Deccan traps (India): insights from dike geochemistry. J Petrol 52(2):315–343
Verwey EJW (1939) Electronic conduction of magnetite (Fe3O4) and its transition point at low temperature. Nature 44:327–328
Wantim M, Suh C, Earns G, Kervyn M, Jacobs P (2011) Characteristics of the 2000 fissure eruption and lava flow fields at mount Cameroon volcano, West Africa: a combined field mapping and remote sensing approach. Geol J 46:344–363
Weinberger R, Levi T, Alsop GI, Marco S (2017) Kinematics of mass transport deposits revealed by magnetic fabrics. Geophys Res Lett 44:7743–7749